



UNIVERSITY OF BRISTOL

NERC INTERNSHIP REPORT

---

# Aerial Photogrammetry for the Earth Sciences

---

*Author:*  
Drew SILCOCK

*Supervisor:*  
Dr Juliet Biggs



Monday 29<sup>th</sup> September, 2014

# 1 Introduction

The aim of this project is to investigate the practical use of photogrammetry, with a focus of its applications to the Earth Sciences. It covers the methods used to gain photogrammetric data and analyses some results taken from fieldwork.

## 1.1 How photogrammetry works

The basic principle of photogrammetry is the same mechanism by which the eyes infer distance: triangulation. By moving around an object, or parallel to a faade, one can infer the distance to the object by a simple trigonometric calculation, as demonstrated in Figure 1. By leveraging this simple trigonometric distance calculation, one can infer from the group of photos of the same object, taken using the appropriate method as described in Section 2.1, the distance to any point in the photos, and thus built up a three dimensional model of the captured objects. Importantly, this can be achieved without need for explicitly inputting the location that the photographs were taken, although it does increase the accuracy of the resulting model, as discussed in Section 2.4.

## 1.2 Unmanned Aerial Vehicles

To gain the photographs and geopositioning data for the photogrammetric reconstruction, we employ the use of Unmanned Aerial Vehicles (UAV). To this end, the ArduPilot Mega (APM)<sup>1</sup> autopilot on-flight hardware and firmware is used. Although a quadcopter is the focus of the research, data was also taken with a hexacopter.

## 1.3 Software Used

### 1.3.1 Mission Planner

Mission Planner<sup>2</sup> was used to interact with and give commands to the APM autopilot. In particular the **survey grid** option, used to guide the UAV in a regular grid pattern, is useful for achieving successful photos for modelling. In addition, Mission Planner is used to geotag the photos. This is discussed in more detail in 2.4.

<sup>1</sup><http://www.ardupilot.co.uk/>

<sup>2</sup><http://planner.ardupilot.com>

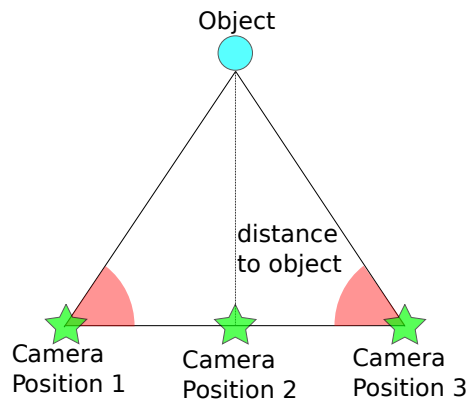


Figure 1: By taking photographs of an object from different angles, one can use trigonometry to calculate the distance to that object.

### 1.3.2 Agisoft PhotoScan

The Agisoft PhotoScan Professional Edition software<sup>3</sup> software is used to perform the photogrammetric reconstruction. The workflow is as follows:

**Load Photos** Firstly, the photos are loaded in PhotoScan.

**Load Camera Positions** Then, the camera geotagging data are loaded, either through importing the photo exif metadata, or through a separate comma separated value file.

**Align Photos** The camera positions are then used to refine the camera position and build a sparse point cloud.

**Place Ground Control Points** Next a mesh is generated and the GCPs are input into PhotoScan.

**Optimise alignment** The camera alignment is then optimised using the GCP data.

**Build Dense Point Cloud** PhotoScan subsequently builds a dense point cloud from the sparse point cloud.

**Build Mesh** Penultimately, the mesh is built by joining the dense point cloud into a smooth model.

**Build Texture** Finally, the mesh is overlaid with a texture, finished the photogrammetric reconstruction.

Once this workflow is accomplished, the resulting model can be exported as an orthophoto, whereby the original photos are stitched together into a single aerial image, and as a Digital Elevation Model (DEM), which contains all the information about the topography of the model. It is this DEM that is of application to Earth Science research.

### 1.3.3 Canon Hack Development Kit

In order to control the camera remotely, we employed the Canon Hack Development Kit (CHDK)<sup>4</sup>. Specifically, we used firmware version 1.00B Alpha for the Powershot IXUS132<sup>5</sup>, loaded by a bootable SD card. This allows one to run scripts on the camera, written in either Lua or UBASIC, that interface with the camera mechanism, e.g. taking pictures, zooming, turning off etc. This allowed us control over the camera during the flights.

---

<sup>3</sup><http://www.agisoft.ru/products/photoscan/professional/>

<sup>4</sup><http://chdk.wikia.com/>

<sup>5</sup><http://chdk.wikia.com/wiki/ELPH115>

## 2 Methods

### 2.1 Photographic Technique

As per the PhotoScan user manual<sup>6</sup>, the photos were taken at an oblique angle to the object being modelled (namely the ground). This amount to ensuring that the camera is facing down towards the ground. This is illustrated in Figure 2.

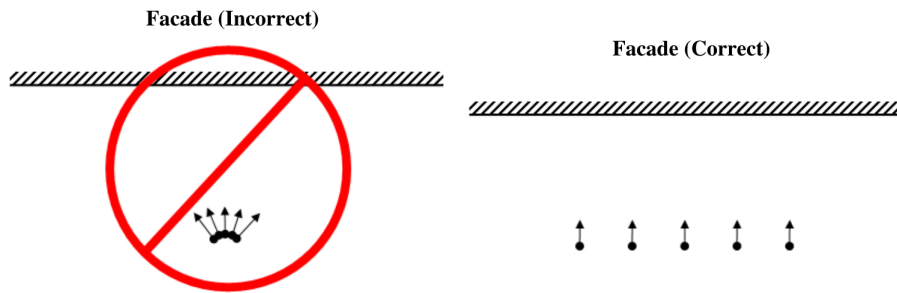


Figure 2: The incorrect and correct method of taking photos useful for photogrammetric modelling, reproduced from the [Agisoft PhotoScan User Manual, Version 1.0](#)

### 2.2 Masking

Occasionally, background or foreground items obstruct the view of the object that one wishes to model, causing error. In these cases, the offending back- or fore-ground objects must be masked out. This means that the photos are individually edited to indicate that part of the photo is not part of the object to be modelled, and should be ignored by PhotoScan when reconstructing the model. A commonly masked element of photographs in photogrammetry is the sky, as is visually shown in Section 4.2.1 and Figure 10. Without masking, the software attempts to integrate the sky into the object being modelled, causing significant error.

### 2.3 CHDK Scripts

#### 2.3.1 Time Interval

The method used predominantly for remote photography is to run a script which automatically takes photos after a regular interval specified by the user. The Lua script for this can be found in Appendix A. To ensure that the photos take at regular intervals, we tested the actual time between photographs, at different

<sup>6</sup>[http://downloads.agisoft.ru/pdf/photoscan-pro\\_1\\_0\\_0\\_en.pdf](http://downloads.agisoft.ru/pdf/photoscan-pro_1_0_0_en.pdf)

input interval values. The results, illustrated in Figure 3, show that below 5 seconds the interval is unreliable. We therefore used 5 seconds as the standard time interval between photos.

### 2.3.2 Pulse Width Modulation Signal

Although it is not used for this research, CHDK scripts can take advantage of the `get_usb_power` function to take input from APM. This utilises Pulse Width Modulation (PWM), whereby repeated short digital signals are interpreted as different voltages due to their high frequency. The APM autopilot send these PWM signals to the camera via a cable, pictured in Figure 4, where the camera interprets them as different voltages. The CHDK script that interprets these voltages, written in UBASIC, is given in Appendix B.

Note that the **Enable Remote** parameter must be enabled under **Settings** → **CHDK Settings** → **Remote Parameters**.

Using the time interval script is in general more practical than taking photos through the CHDK cable using PWM. This is because the time interval method is as simple as strapping the camera to the copter and setting to photographing, whereas when using the CHDK cable, one needs to either set APM to take photos at every waypoint using MP, which one cannot do when controlling the UAV manually, or assign the camera ‘shoot’ functionality to a button on the radio control system, in which case one needs to press this button every few seconds.

## 2.4 Geotagging

In order to increase the accuracy and precision of the camera location in

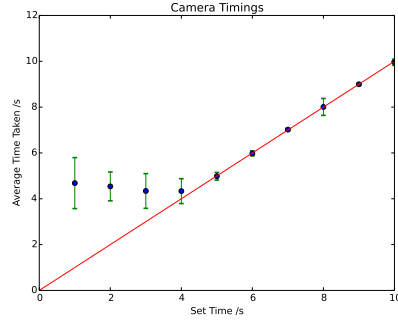


Figure 3: The measured averaged time difference between successive photos, plotted against the interval input into the script. 11 photos, giving 10 time differences, were taken.

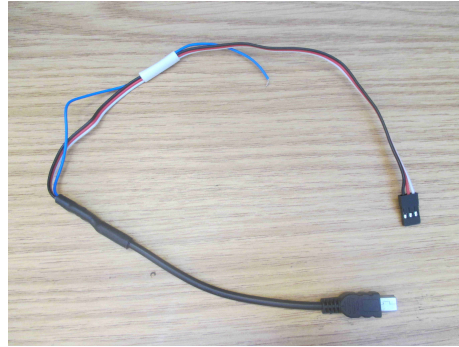


Figure 4: The cable used to connect the camera running CHDK to the APM board. PWM signals are sent through this cable and interpreted by scripts running on the camera

the photogrammetry software, and thereby the accuracy and precision of the final model, the photos are tagged with their location by using the UAV's on-board Global Positioning System (GPS). The geolocation is written either into a separate comma separated value (CSV) file, or is written directly into the exif metadata of the photos themselves. Either can be imported into PhotoScan. The technique used to determine the location of the photographs depends on whether the photographs were taken using the time interval script or as controlled by the APM autopilot.

#### 2.4.1 Time Offset Method

If the camera is set to automatically take pictures every 5 seconds, then one needs to know the difference between the internally logged time on the camera, stamped onto the photographs' exif metadata by the camera automatically, and the GPS time on the UAV. As the UAV constantly takes logs of its GPS location and the time, knowing the time difference between camera and GPS is sufficient to determine the location of each of the photos. Inputting the log, photographs and time difference into MP, MP automatically geotags the photos to be imported into PhotoScan.

In order to find this time difference, a photograph of MP while connected directly by USB to the APM, as illustrated in Figure 5, is taken. As the UAV GPS time is displayed on the MP screen, and the camera logs the time it takes the photograph, comparing the exif time stamp to the GPS time recorded in the photo itself gives the time difference.

#### 2.4.2 CAM Dataflash Log Messages

If using the UBASIC CHDK script given in Appendix B to allow APM to remotely trigger camera shooting, then the GPS time, location, altitude, roll, pitch and yaw are all logged by APM. A line will appear in the dataflash log of the form:

CAM, GPSTime, GPSWeek, Lat, Lng, Alt, Roll, Pitch, Yaw

Geotagging the photos using the CAM messages embedded in the dataflash logs is the more accurate method, as there are no uncertainties introduced by the time logged by the camera.



Figure 5: A photograph taken of MP while connected directly to the APM, giving the offset between the camera time and the UAV GPS time.

### 2.4.3 Shutter Lag

If using the CAM message method, the lag between the instruction to shoot and the photograph being actually taken, induced by shutter lag, can cause systematic errors in the geotagging and must be measured so that it can be taken into account. To quantify this, we analysed the shutter lag of the Powershot IXUS132 we are using. This involved taking a photo of a timer<sup>7</sup> exactly on the second, and noting the time shown in the photograph. We calculated the shutter lag to be  $(90.3 \pm 32.0)$ ms excluding the autofocus lag, and  $(341 \pm 140.3)$ ms including the autofocus lag. As the camera is not set to autofocus using this method of remote photography, the former value is taken as the value of interest. As the GPS logs are made only at a frequency of 5 Hz (or one every 200 ms)<sup>8</sup>, the shutter lag is rounded to the nearest 200 ms and taken as zero.

## 2.5 Ground Control Points

To enhance the accuracy and precision of the reconstructions, we employed Ground Control Points (GCPs). These are strategically placed markers, the exact location of which are surveyed and subsequently input into PhotoScan. Then, in PhotoScan, after the cameras are aligned, inputting the GCPs as markers and giving their geolocation (either preferably as WGS or possibly also as local coordinates) allows one to optimise the alignment of the cameras, producing a more accurate dense point cloud and therefore textured model.

Distinguishable points such as dark crosses are preferable, as they are easier to pick out on photos when creating markers in PhotoScan, and easier for PhotoScan to analyse and pick out the location of in each picture. I particular crosses are effective as the exact location of the marker can be precisely set to the centre of the cross.

As per the PhotoScan website<sup>9</sup>, roughly 10 GCPs are required for the completion of the georeferencing, while 15 or more GCPs are preferable for improved accuracy.

The laser-based surveying equipment used to identify the GCPs is shown in Figure 6.

## 3 Theory

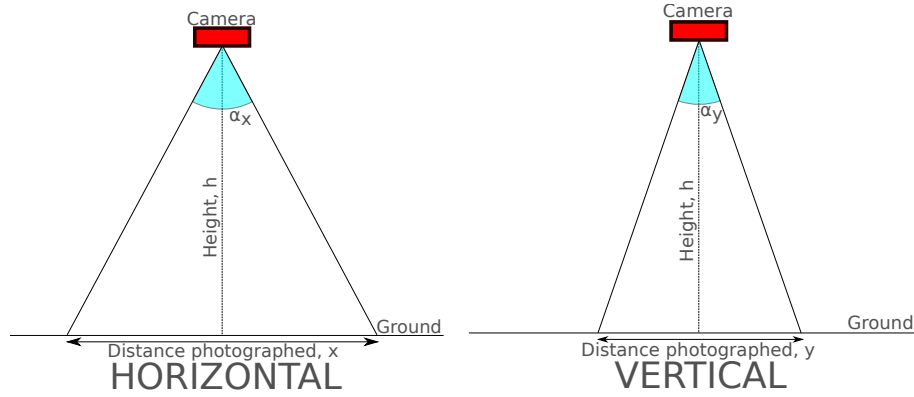
### 3.1 Calculating Resolution as Function of Height

---

<sup>7</sup><http://edwardns.com/shutterlag.html>

<sup>8</sup>As per [http://copter.ardupilot.com/wiki/common-geotagging-images-with-mission-planner/#Geotag\\_Mode](http://copter.ardupilot.com/wiki/common-geotagging-images-with-mission-planner/#Geotag_Mode) and <https://store.3drobotics.com/products/3dr-gps-ublox-with-compass>

<sup>9</sup>[http://www.agisoft.ru/wiki/PhotoScan/Tips\\_and\\_Tricks#Ground\\_Control](http://www.agisoft.ru/wiki/PhotoScan/Tips_and_Tricks#Ground_Control)



(a) The horizontal view of the angle of view of the camera facing the ground. (b) The vertical view of the angle of view of the camera facing the ground.

Figure 7: The views of the angle of view as the camera faces directly towards the ground.

If one knows the resolution of the camera, the height from which the photo was taken and the angle of view of the camera, then one can calculate the resolution of the resulting photographs, in terms of how many meters correspond to a single pixel.

To do this, the geometry of the situation, illustrated in Figure 7, is parametrised as follows:

- Distance photographed along ground:  $x$  and  $y$
- Resolution of camera (n# pixels):  $r_x$  and  $r_y$
- Height from which photo was taken:  $h$
- Angle of view of camera:  $\alpha_x$  and  $\alpha_y$
- Number of meters corresponding to a single pixel:  $\mu_x$  and  $\mu_y$

Then according to this parametrisation, as a matter of elementary trigonometry:



Figure 6: The equipment used to survey in Ground Control Points.



$$\tan\left(\frac{\alpha_x}{2}\right) = \frac{x}{2h} \text{ and} \quad (1)$$

$$\tan\left(\frac{\alpha_y}{2}\right) = \frac{y}{2h} \quad (2)$$

$$(3)$$

Rearranging this for  $x$  and  $y$  gives:

$$x = 2h \tan\left(\frac{\alpha_x}{2}\right) \text{ and} \quad (4)$$

$$y = 2h \tan\left(\frac{\alpha_y}{2}\right) \quad (5)$$

Then the resolution in meters per pixel is simply this distance  $x$  divided by the total number of pixels in the photograph:

$$\mu_x = \frac{x}{r_x} = \frac{2h \tan\left(\frac{\alpha_x}{2}\right)}{r_x} \text{ and} \quad (6)$$

$$\mu_y = \frac{y}{r_y} = \frac{2h \tan\left(\frac{\alpha_y}{2}\right)}{r_y} \quad (7)$$

This agrees approximately with the values generated by PhotoScan in doing the photogrammetric reconstruction, discussed in Sections 4.1.2 and 4.2.3.

### 3.2 Ensuring sufficient photo overlap

Agisoft states in the PhotoScan User Manual<sup>10</sup> that 80% overlap is needed for standard front overlap between successive photos. Thus, one can calculate the speed one needs to travel at to ensure that if one takes photos every five seconds, the overlap is at least 80%.

The distance between the photo locations, illustrated in Figure ??, is then given by:

$$d_{int} = 2h \tan\left(\frac{\alpha_y}{2}\right) - \text{overlap} \quad (8)$$

$$= 2h \tan\left(\frac{\alpha_y}{2}\right) - 2h\omega \tan\left(\frac{\alpha_y}{2}\right) \quad (9)$$

$$= 2h \tan\left(\frac{\alpha_y}{2}\right) [1 - \omega] \quad (10)$$

Where  $d_{int}$  is the required maximum distance between the photos needed to ensure an overlap of  $\omega$ , where the vertical angle of view is  $\alpha_y$  and the photographs

---

<sup>10</sup>PhotoScan 1.0.0 user Manual, “Capturing Scenarios”, Page 5. [http://downloads.agisoft.ru/pdf/photoscan-pro\\_1\\_0\\_0\\_en.pdf](http://downloads.agisoft.ru/pdf/photoscan-pro_1_0_0_en.pdf)

are taken from a height  $h$ . For the Ixus 132 we used with  $\alpha_y = 48.9^\circ$ , requiring an overlap of  $\omega = 0.8$  gives:

$$d_{int} = 0.182h \text{ meters/second} \quad (11)$$

If the photos are taken once every five seconds ( $t_{int} = 5$  seconds), as we did, then this gives a maximum UAV velocity of:

$$v_{UAV} = \frac{d_{int}}{t_{int}} = 0.0364h \text{ meters/second} \quad (12)$$

Taking a reasonable height of  $h = 50$  meters thus gives:

$$v_{UAV} = 1.82 \text{ meters/second} \quad (13)$$

This is a very reasonable and achievable speed.

## 4 Results

Two sets of data were taken, and are examined here in terms of the accuracy of their produced models and the possible causes of error in the reconstruction process. The first set of photographs were taken at Long Ashton Farm outside Bristol, and the second set were taken at the Avon Gorge in Bristol.

### 4.1 Long Ashton

For this data set, a hexacopter was used to gather a total of 63 aerial images. The time interval technique was used to take the photos, and the time offset method used to geotag the resulting photos.

#### 4.1.1 Without GCPs

Firstly, the reconstruction was run without the Ground Control Points input, and without any photographic alignment optimisation. The resulting orthophoto is shown in Figure 8a, while the DEM is shown in Figure 8b and the photographic overlap is shown in Figure 8c. The produced model is available to [view interactively online](#).

Clearly, the orthophoto shows that the 63 photos were sufficient to build a model of the topography of the area. However, the Digital Elevation Model shows that the photogrammetric reconstruction interpreted the topography as on a significant tilt head from the car park up to the building. We hypothesise that this tilt is due to the lack of GCPs to correct for such systematic errors. This is discussed with reference to the model produced *with* GCPs in Section 4.1.2 and also with reference to the Avon Gorge reconstruction in Section 4.2.

Figure 8c shows that the overlap between the photos is more than adequate in all the central areas of the model, only reducing to  $<9$  around the very edges of the area.

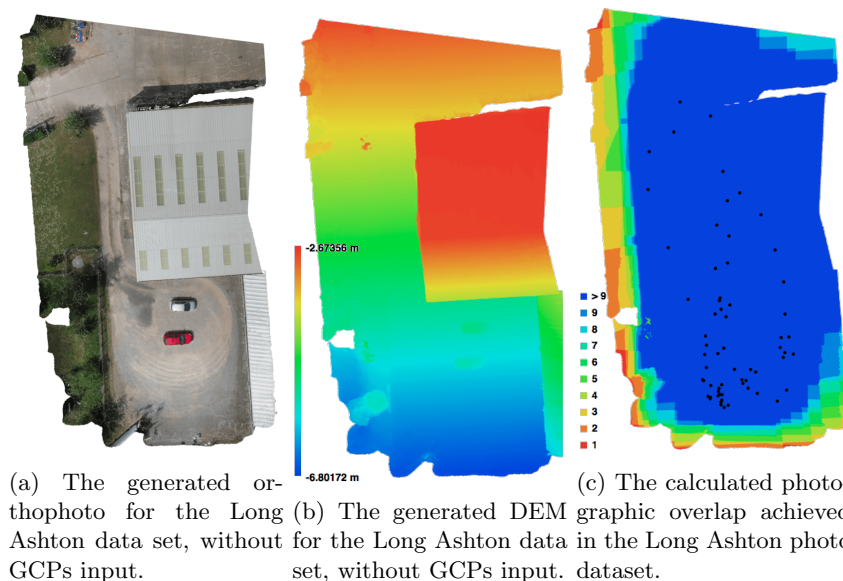


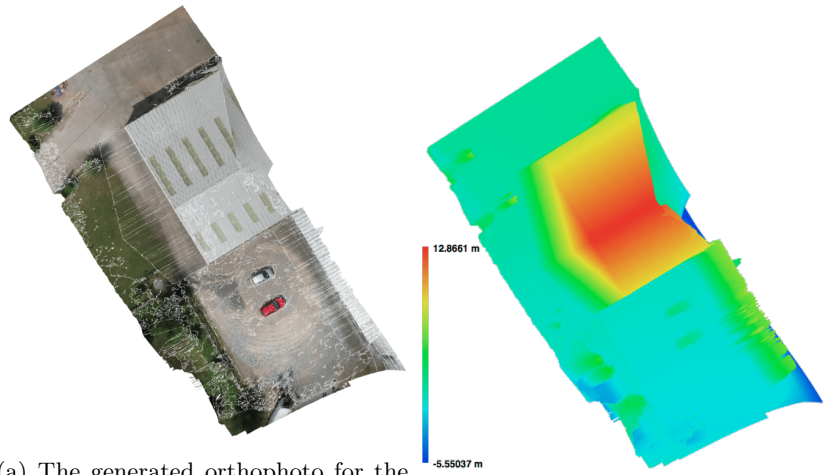
Figure 8: The data produced by PhotoScan from the Long Ashton aerial imagery, without factoring in GCPs.

#### 4.1.2 With GCPs

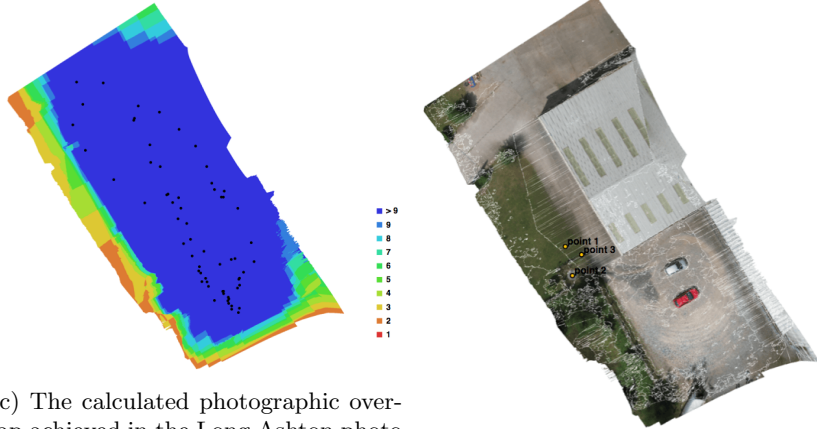
The reconstruction was then rerun with a limited number of Ground Control Points input. These GCPs were taken using distinguishable features from the landscape and their geolocation found from Google Earth to test the effect they would have on the resulting model and DEM. The first DEM was taken as the centre of a pond, the second the corner of a fence and the third was a cross marked in with white tape, whose location was approximated by referencing nearby features on Google Maps. While this is not sufficiently accurate for a true georeference, it suffices to demonstrate that the tilt is removed from the final model once the GCPs are introduced.

Figure 9b shows the DEM with these 3 GCPs introduced into the photogrammetric alignment process. Clearly, the model is no longer considering on a slope, as it was in Figure 8b. However, the previously vertical faces are now tilted themselves, meaning that the wall of the warehouse is not vertically up, but a tilted slope up to the roof. We argue that this is an artefact of the small number of GCPs used trying to georeference the model. If the minimum number of 10 GCPs or more were used, then the software would correctly georeference the model and the sloped walls would be corrected. Section 4.2.2 and 4.2.3 discusses this further with reference to the Avon Gorge photo set, which contained more than the required number of GCPs.

The data generated by PhotoScan, displayed in Table 1, further illustrates the inefficacy of georeferencing with geotagged photos alone. Not only does



(a) The generated orthophoto for the Long Ashton data set, with 3 GCPs input. (b) The generated DEM for the Long Ashton data set, with 3 GCPs input.



(c) The calculated photographic overlap achieved in the Long Ashton photo dataset with 3 GCPs. (d) The locations of the placed GCPs.

Figure 9: The data produced by PhotoScan from the Long Ashton aerial imagery, with 3 GCPs input.

	Without GCPs	With GCPs
<b>Flying Altitude</b> (m)	4.88261	37.1183
<b>Ground Resolution</b> (m/pix)	0.000940159	0.00622731
<b>Error</b> (pix)	0.971366	1.37699
<b>DEM Resolution</b> (m/pix)	0.00376064	0.0249093

Table 1: The data generated by PhotoScan for the Long Ashton models, with and without GCPs.

the final model appear slanted, but the flying altitude is incorrectly taken to be 4.9m. Even with only 3 GCPs, this altitude error is corrected when the GCPs are used to georeference the model as well as the geotagged photos. This difference in calculated flying altitude also explains the better ground and DEM resolution for the model reconstructed without GCPs as opposed to the model reconstructed with the GCPs; the factor by which the GCP ground and DEM resolution is better is approximately equal to the factor by which the GCP model flying altitude is higher, taking the slight difference in error into account. Having a higher flying altitude means each pixel corresponds to a larger distance.

The errors for both models are approximately equal at  $\approx 1$  pix, with a slightly higher error for the model with GCPs. This number represents the root means square reprojection error calculated over all features points detected on the photo. Thus, a possible source of the error is that without the GCPs, the software is unaware of the systematic error demonstrated by the sloped DEM. When the GCPs are introduced, the software realises that the systematic error is there, and the value of the reprojection error is increased accordingly. Even though the GCP georeferenced model has a slightly larger error, it still corresponds to a very small distance of 0.155 mm. This value is too small to be a realistic value, indicating that the GCPs have not sufficiently corrected the model to its true value for the error present in the model to be recognised and reported by PhotoScan. This is supported by the comparison in Section 4.2.3.

## 4.2 Avon Gorge

This model was reconstructed from two passes of 87 and 61 photos. As before, the time interval with time offset techniques were used for taking photos and geotagging the photos, respectively. The photos were taken by attaching the camera to the quadcopter and tilting it by hand to attain horizontally oriented photographs of the cliff face that is the Avon-Gorge. The purpose of this was to give useful photos equivalent to aerial photogrammetry before the quadcopter was ready to fly.

### 4.2.1 First Pass Versus Second Pass

The first pass was taken facing the gorge horizontally on, thereby fully representing an equivalent to aerial photogrammetry. The second pass was at an

oblique angle, facing upwards to capture the top of the gorge. As expected, the second pass at an oblique angle produced less accurate results than the first pass at a zenithal angle to the cliff face. This is shown visually in Figures 10a and 10b. In particular where the oblique angle causes the camera to be unable to see the top of the cliff and where the cliff meets the sky, the model is erroneous. For the former the model produces clear spikes in the model, jutting from the face of the cliff. For the latter, the software includes the sky as an extension of the cliff. Masking the sky out, as described in Section 2.2, removes the latter problem to a limited extent, but the former remains, as shown in Figure 10c.

#### 4.2.2 Without GCPs

When the first pass is taken with no GCPs input, there are several important emergent features to note.

Firstly, as Figure 11d shows, the calculated locations of the cameras was very inaccurate, with some errors extending beyond the model. This is because the geolocation of the photos from the on-board UAV GPS is simply not accurate enough to be the only method of georeferencing; the GCPs are also needed in addition to the geotagged photo locations.

Secondly, as Figure 11b shows, the reconstruction has also incorrectly interpreted the landscape as being on a tilt, with the north of the gorge (top of the image) appearing higher than the south of the gorge (bottom of the image). The systematic sloping that these reconstructions seem to exhibit is a strange if irrelevant phenomenon (so long as a sufficient number of GCPs are provided), possibly caused by the camera being tilted as it is attached to the UAVs.

#### 4.2.3 With GCPs

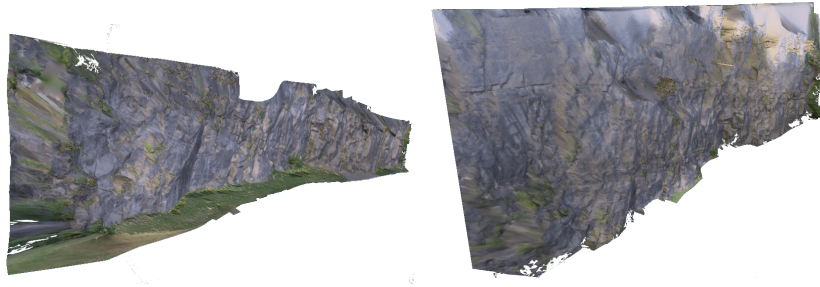
Once the GCPs are input, there are several important effects.

The photographic overlap of the gorge increases, with only the very corners having less than 9 overlapped photos covering it. With more accurate georeferencing, the software recognises the photos as taken more spread apart, and thus with better coverage of the corners of the model.

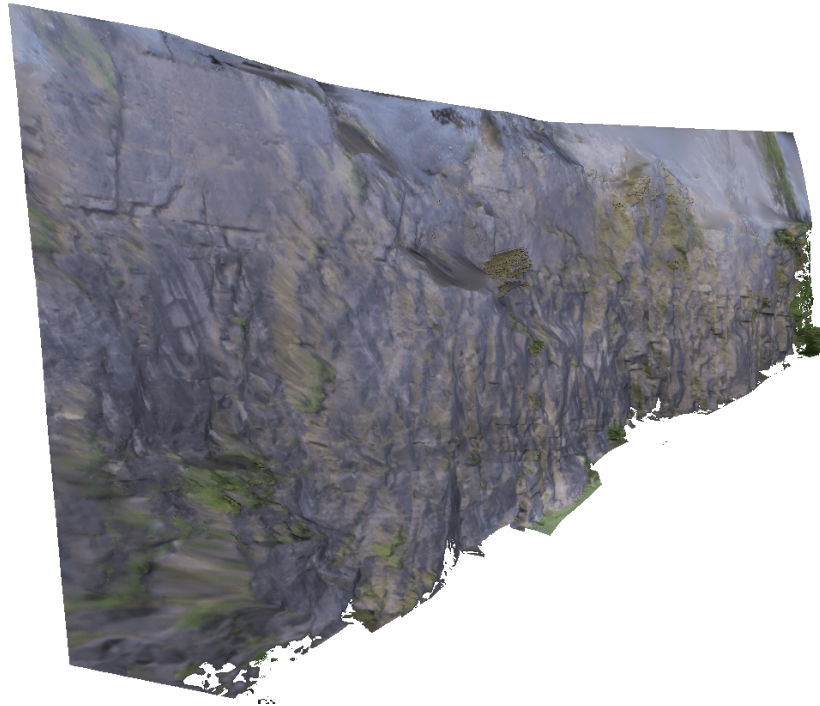
The tilt present in Figure 11b disappears, as shown in Figure 12b. The produced model now correctly identifies the bottom of the gorge as level. This indicates that the slopes present in the Avon Gorge and Long Ashton models are merely artefacts of the lack of GCPs, which, when the sufficient number of GCPs are introduced, disappears.

The data produced by PhotoScan is shown in Table 2. As in Table 1, the flying altitude is increased significantly for the GCP georeferenced model, although in this context the flying altitude has less meaning owing to the fact that the photographs of the gorge were taken horizontally. As before, the ground resolution is better, again due to the different value of the flying altitude inferred from the software.

The difference in reprojection error is more pronounced here, which could be explained by the higher number of GCPs; with the model fully accurately



(a) The model produced using only the first pass of photos at the zenithal angle. (b) The model produced using only the second pass of photos at the oblique angle.



(c) The model produced using only the second pass of photos, masking out the sky.

Figure 10: A visual comparison of the relative error induced in the models produced in the first and second passes, at zenithal and oblique angles respectively.

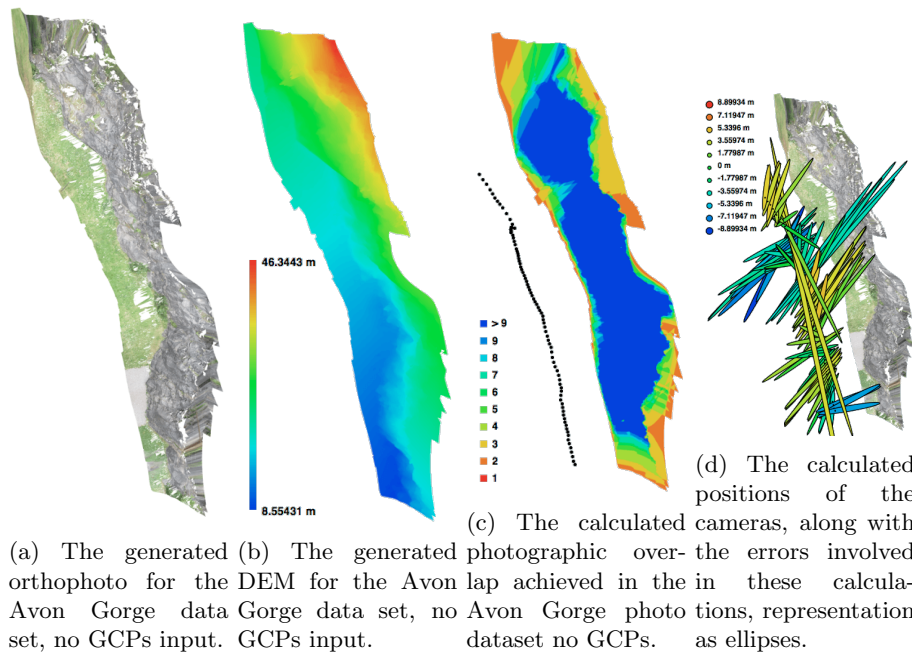
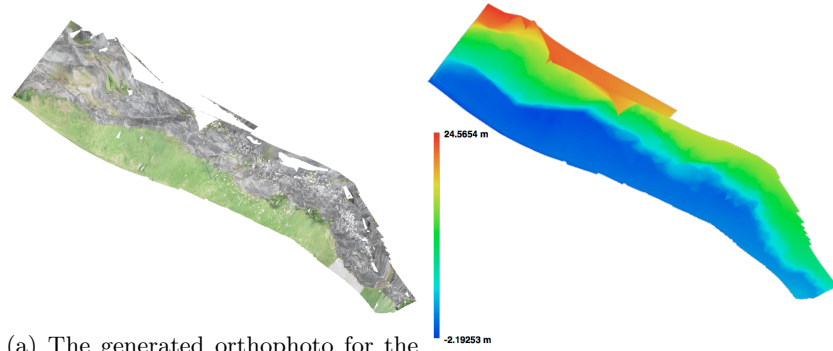
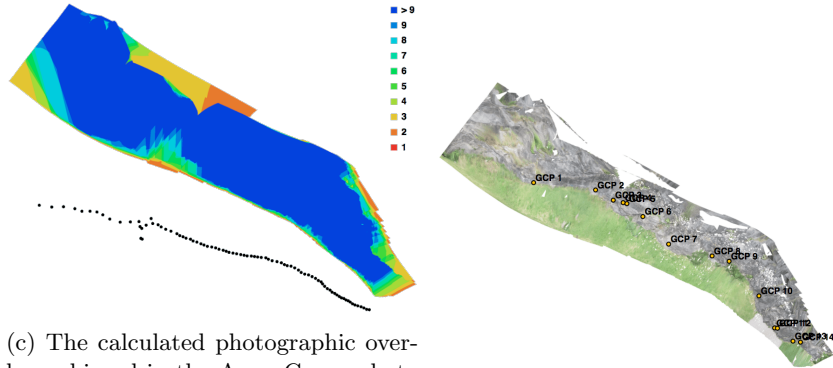


Figure 11: The data produced by PhotoScan from the Avon Gorge horizontal imagery, no GCPs input.





(a) The generated orthophoto for the Avon Gorge data set, with 14 GCPs input. (b) The generated DEM for the Avon Gorge data set, with 14 GCPs input.



(c) The calculated photographic overlap achieved in the Avon Gorge photo dataset with 14 GCPs. (d) The positions of the input GCPs.

Figure 12: The data produced by PhotoScan from the Avon Gorge horizontal imagery, with 14 GCPs input.

	Without GCPs	With GCPs
<b>Flying Altitude</b> (m)	16.5655	51.5781
<b>Ground Resolution</b> (m/pix)	0.00339199	0.00260205
<b>Error</b> (pix)	1.02017	4.76105
<b>DEM Resolution</b> (m/pix)	0.013568	0.0692152

Table 2: The PhotoScan generated data for the Avon Gorge models, with and without GCPs.

georeferenced, the errors in the reprojection are fully realised and reported by PhotoScan, meaning that the reported error is higher. It’s important to note that, as before, even the higher value of the error for the GCP georeferenced model, which corresponds to a value in meters of 1.24 cm, is well within an acceptable range. The fact that this value is also realistic indicates that the previously unrealistically small error in Section 4.1.2 was indeed a result of not having enough GCPs to properly georeference the model, thereby resulting in PhotoScan not fully recognising the error present in the model.

## 5 Conclusion

In conclusion, aerial photography can provide an accurate 3-dimensional photogrammetric reconstruction of the topology of the ground, and a useful corresponding DEM, with an error on the scale of a few centimetres. This is sufficiently accurate to be able to produce useful DEM for geological purposes. Importantly, this accuracy can only be achieved using both geotagged photos and Ground Control Points for the georeferencing. Without the GCPs, the models exhibit systematic error such as the tilts discussed in Sections 4.1 and 4.2.

## 6 Future Projects

The following are proposals for future research into this field:

- Assess the relative accuracy achieved by using the CAM geotagging method as opposed to the time interval CHDK script.
- Further investigate the possible applications of photogrammetry to different areas of Earth Science.

## 7 Appendices

### A Time Interval CHDK Script

The script used to take pictures every 5 seconds is as follows:

```
--[[
@title Intervalometer
@param a = interval (sec)
@default a 5
@param b = number of photos
@default b -1
--]]
repeat
    start = get_tick_count()
    shoot()
    sleep(a*1000 - (get_tick_count() - start))
    b = b - 1
until (b = 0)
```

This is adapted from the default `interval.lua` script, packaged with all versions of CHDK under the `SCRIPTS` directory. Note that there are two parameters: `a` is the time interval between successive photos, in seconds, which we set to 5, and `b` is the number of photos to take in total. By default, this is set to -1, meaning it will continue taking photos indefinitely, however it can be useful to limit the number of photos.

## B Pulse Width Modulation CHDK Script

The script used to control the camera functions remotely through the CHDK cable using PWM is shown below. It is taken directly from the APM wiki page on CHDK camera control<sup>11</sup>.

```
@title 3DR Shooter
rem author Brandon Basso, 3D Robotics
rem author Dave Mitchell - dave@zenoshrdlu.com
rem This script is based on the basic Gentled CHDK2 script
rem It takes pictures and sets zooms to a few different levels

@param o Zoom-extended
@default o 100
@param i Zoom-stowed
@default i 30
@param s Zoom-shoot
@default s 10

while 1
  do
    k = get_usb_power
    until k>0
      if k < 5 then gosub "ch1up"
      if k > 4 and k < 8 then gosub "ch1mid"
      if k > 7 and k < 11 then gosub "ch1down"
      if k > 10 and k < 14 then gosub "ch2up"
      if k > 13 and k < 17 then gosub "ch2mid"
      if k > 16 and k < 20 then gosub "ch2down"
      if k > 19 then print "error"
    wend
  end

:ch1up
  print "Ch1Up-Shoot"; k
  set_zoom s
  shoot
  sleep 1000
  return

:ch1mid
  print "Ch1Mid-Stowed"; k
  set_zoom i
  sleep 1000
```

---

<sup>11</sup><http://plane.ardupilot.com/wiki/common-chdk-camera-control-tutorial/>

```

    return

:ch1down
    print "Ch1Down-Extended"; k
    set_zoom o
    sleep 1000
    return

```

The variable `k`, set equal to the current power going into the camera through the USB port, corresponds to different pulse widths as given by Table 3<sup>12</sup>.

Pulse Width (ms)	get_usb_power
1,900	<5
1,500	>4 and <8
1,100	>7 and <110

Table 3: The conversion between PWM widths and the value taken from `get_usb_power`.

---

<sup>12</sup><http://plane.ardupilot.com/wiki/common-chdk-camera-control-tutorial/>

## C Models

All of the photogrammetric models discussed in this report, along with many others, are available to view online at:

<https://sketchfab.com/drewsberry/models>

In particular, the following discussed models are available for viewing:

**Long Ashton Without GCPs:**

<https://sketchfab.com/models/ec777be4b73f4e7a8fdd992c2b8d026a>

**Long Ashton With GCPs:**

<https://sketchfab.com/models/deaac286092b48498ef24cf6cae55b5f>

**Avon Gorge Pass 1 No GCPs:**

<https://sketchfab.com/models/ad8a1d9f8c324eb592a9e4beabc5a51e>

**Avon Gorge Pass 2 Unmasked No GCPs:**

<https://sketchfab.com/models/2a51ae61e6bd4157bca421ab9c0c6b9f>

**Avon Gorge Pass 2 Masked No GCPs:**

<https://sketchfab.com/models/6b531108db5040e297ada8d9912391b3>

**Avon Gorge Passes 1 and 2 Unmasked No GCPs:**

<https://sketchfab.com/models/a9bdb7de52f24a7c8b5138259620ec93>

**Avon Gorge Passes 1 and 2 Masked No GCPs:**

<https://sketchfab.com/models/0240057c321a44cf9a8c468372675b39>

**Avon Gorge Pass 1 With GCPs:**

<https://sketchfab.com/models/f277a6c6f6984ed1ad804d1afdaf35e3>